NASA TECHNICAL
MEMORANDUM

NASA TM X- 68189

INSTANTANEOUS DISTORTION INVESTIGATION

by James E. Calogeras
Lewis Research Center
Cleveland, Ohio 44135

INSTANTANEOUS DISTORTION INVESTIGATION

by James E. Calogeras

Lewis Research Center
National Aeronautics and Space Administration
Cleveland, Ohio

INTRODUCTORY REMARKS

The purpose of this presentation is to review some of the results obtained in an inlet-engine compatibility test run in the 10x10 SWT of the NASA-Lewis Research Center. This program was run to measure the time-variant distortions produced in a supersonic inlet and to relate a unique distortion peak, occurring in an instant of time, to the origin of stall in a compressor. The major stumbling block in this type of effort is the determination of a proper increment of time over which to average pressures before computing distortions. It is reasonable to expect that the proper averaging time is related to the particular compressor in question. Indeed, some results of similar investigations have indicated that the proper averaging time was solely dependent on the response characteristics of the compressor. Nonetheless, the most significant point in this presentation is that the proper averaging time may not be solely dependent on a particular compressor, and, in fact, may vary with operating conditions, even for the same inlet-engine combination.

APPARATUS AND PROCEDURE

Figure 1 shows the installation of the inlet combined with a coldpipe-choked plug assembly in the test section of the 10x10 foot SWT. The inlet was an axisymmetric mixed-compression type designed for Mach 2.5. Sixty percent of the supersonic compression was done externally. It has a translating centerbody to effect restart and off-design operation, fast-acting bypass doors for terminal shock control, and provisions for both bleed and vortex generators on cowl and centerbody surfaces for boundary layer control.

The engine used in the compatibility study was a J85-GE-13 turbojet. It consists of an eight-stage axial-flow compressor coupled directly to a two-stage turbine. The exhaust nozzle area was manually controlled for this investigation. The compressor was stalled by slowly closing the nozzle while maintaining a constant engine speed. In order to avoid over-temperaturing the turbine during this procedure, the first stage turbine nozzle was 14 percent smaller in area than the standard unit. At any point on the compressor map, then, the turbine was matched to the compressor at a lower turbine inlet temperature.

Steady-state and dynamic pressure instrumentation at the compressor face and compressor discharge stations is presented in figure 2. Only the fluctuating component of pressure was recorded from each of the dynamic probes. This component was later added to the time-averaged (steady-state) pressure provided by the adjacent probe. Frequency response of the dynamic compressor face probes was flat to about 2000 Hz. Response of the compressor discharge dynamic

pressure probes, as well as two rows of interstage static probes not shown in this figure, was flat to about 300 Hz. The fluctuating component of each pressure transducer was recorded on FM-multiplexed tape at a recording speed of 60 inches per second. This speed provided recording capability of up to 4000 Hz.

Figure 3 illustrates the data acquisition and reduction scheme used in this investigation. The acquisition portion of the figure has already been discussed. The demultiplexed tape was played back through low-pass filters at a playback speed 1/16th of the record speed. This allowed simultaneous digitizing of each of the compressor face probes at an effective rate of 8000 samples/sec/channel, for at least five samples per cycle of the highest frequency content left in the data. It should be noted that the pre-digitizer filters were six-pole types, and with an effective 1600 Hz cutoff frequency, represented a true average of data corresponding to about 1/4th of a milli-second. So even if distortion was calculated and plotted every 1/8th milli-second for a time period just prior to compressor stall, each calculation would represent a distortion averaged for about 1/4th millisecond. This corresponds to about 22° of rotor rotation.

Distortion computations were made on an IBM 7090 computer after super-imposing the steady-state levels of each compressor face total probe. Format of the reduced data was in either printed digital output or microfilm plots.

RESULTS AND DISCUSSION

Figure 4 outlines the screening process of data recorded in the compati-bility study. A total of 29 stall points were recorded on FM-multiplexed tape. These stalls occurred at free-stream Mach numbers of 2.5 and 2.6, at angles-of-attack from 0° to 7°, at engine corrected speeds from 86 to 100 percent of rated speed, for inlet configurations with and without vortex generators, and for bypass flows from 3 to about 20 percent of capture airflow. Of the total 17 stalls were of the "drift" type. That is, all facility and model operating conditions had been set and had reached equilibrium when the compressor abruptly stalled. Of these, the cycle time of the steady-state recording system limited the recording to 11 stall points. This was the number of points digitized. Of the digitized points, two stalls occurred with relatively low levels of both steady-state and time variant distortion. Predictably, these stalls occurred on the undistorted stall line of the compressor map. Two other points did lose significant amounts of stall margin. But these losses were all attributed to respective levels of steady-state distortion. So of the 29 stall points recorded on tape, the conditions of only 7 were favorable for analysis on a time-variant basis.

The sensitivity of the compressor to various types of distortion patterns is presented in figure 5. These results are from a screen-induced distortion program run with the same engine used in the wind tunnel test. Loss in compressor pressure ratio at stall is plotted as a function of a distortion index based on a critical angle of spoiled flow. The P_{min}, 60° used in this figure was defined as the lowest mean pressure in any 60° sector of a flow

annulus. For those cases with full-span circumferential distortion, the flow annulus was the compressor face annulus. For the other cases represented in this figure, as well as for the stall points recorded in the wind tunnel program, the compressor face was divided into equal-area rings, and the distortion computed in each of these rings. Averaging across a 60° sector was done to account for the dynamic response of the compressor to spoiled flows less than 60° in circumferential extent. This response was not predictable by the classical method of parallel compressor theory. By applying this correlation to each of the digitized stall points recorded in the wind tunnel program, the recorded compressor pressure ratio at stall furnished the critical level of distortion required to stall the compressor. This is demonstrated in the next figure.

In figure 6 the same distortion index shown in the previous figure is applied to a typical wind tunnel stall point on a time-variant basis. The distortion computations were made and plotted every 0.125 millisecond for a period of almost 50 milliseconds prior to the complete breakdown of flow in the compressor (terminal stall). The averaging time of 0.072 rotor revolution represents the effective averaging time of the pre-digitizer filters. The stall hammershock corresponds to the rapid rise in compressor face total pressure resulting from compressor terminal stall. Notice that in this case, evidence of compressor stall was observed inside the compressor a full 6 milliseconds before it became evident with compressor face instrumentation. It is this earliest time to which a unique instantaneous distortion peak should be related.

Definition of the three distortion levels indicated by dashed lines is as follows:
1. The steady state distortion level is that calculated using steady-state pressures. Notice that the average level of time variant distortion is well above the steady-state distortion level. This is because of the short pressure averaging time used in these time-variant distortion calculations. As this averaging time increases, the average level of time-variant distortion will approach the steady-state level.

2. The critical level is that furnished by the steady-state correlation of the previous figure. It is the amount of distortion it should have taken to cause the compressor to stall at the measured pressure ratio. In this sample, the critical level is more than three times the steady-state level. And there are at least five distortion peaks which approach or exceed this level in a period prior to the origin of stall corresponding to only about ten revolutions of the rotor.

3. The instantaneous distortion level is that exceeded by no more than a single distortion peak. By definition then, when the ratio of instantaneous to critical distortions equals unity, there will exist a single distortion peak which equals or exceeds the critical level of distortion. In this sample, the instantaneous to critical distortion ratio is 1.26. By increasing the pressure averaging time, this ratio will reach unity. It then remains to be seen if the unique distortion peak which results can be related to the origin of stall in the compressor.

The ratio of instantaneous-to-critical distortions is presented in figure 7 as a function of pressure averaging time for three of the seven digitized stall points which were analyzed. For each of the readings, the intersection of the curve faired through the symbolled points with the instantaneous-to-critical distortion ratio of unity represents the proper averaging time. Because of the definition of the instantaneous distortion level, the locus of points for reading 3 never does intersect the distortion ratio of unity. But a subsequent figure will show that, for this reading, the proper averaging time corresponds to about 0.07 rotor revolutions.

The range of "proper" averaging times shown in this figure (0.07 to 1.4 rotor revolutions) includes all of the seven stall points analyzed. The mean averaging time was 0.43 rotor revolutions, although only two of the seven points exceeded this value. The wide variation in averaging time may be explained in part by basic differences in distortion types. For example, the compressor may respond in a completely different manner to a radial distortion pattern in which "holes" of low-pressure air appear in the high pressure regions than, say, to a largely circumferential distortion pattern which maintains its basic shape regardless of the pressure fluctuations. Another possible explanation for variations in averaging time is that the distortion calculation itself takes no account of the circumferential location of the low pressure zone. Hence, the proper averaging time for a stall point in which the location of the spoiled zone varies randomly with time may again be quite different than that for a point in which the location remains fixed. And finally, some variation in averaging time is to be expected, if only because of the data scatter associated with the steady-state distortion correlation.

Steady-state total pressure contours for reading 2 are presented in figure 8. Each shaded area of the map represents a given range of total pressure recovery, with the darkest region representing the lowest recovery. The boundary between any two shaded regions is a constant pressure contour.

The data of reading 2 were recorded at Mach 2.5 with the inlet at 0° angle-of-attack. Consequently, the distortion is almost purely radial, with the lowest pressure region occurring at the hub. However, the highest dynamic activity occurred in the higher pressure region for this point, causing zones of low pressure to appear and disappear in the good flow. The result is shown in the next figure.

Figure 9 shows the time variation of distortion for reading 2 for a 50-millisecond period prior to and including the terminal stall of the compressor. The averaging time used in this figure is just slightly less than the proper averaging time determined in a previous figure. Notice that the steady-state distortion for this point is quite low, far below the critical level predicted by the correlation. This is due to the almost purely radial nature of the steady-state distortion pattern. But on a time-variant basis, the "holes" appearing in the regions near the blade tips cause large amplitude fluctuations of distortion in these regions. And approximately 1 millisecond prior to the observation of stall inside the compressor, the instantaneous distortion traverses beyond the critical level. Because of the physical size of the

J85 compressor and the proximity of the compressor face probes, 1 millisecond is about the time it would take to transport a distortion into the compressor and break down the circulation about its blades. So while other distortion peaks approach the critical level and one even exceeds it in the span of time shown here, it is most probable that the single highest distortion peak nearest the stall observation time induced the compressor to stall.

One of the more interesting aspects of this figure is the 12 millisecond time delay between the initial observation of stall inside the compressor and the first evidence of that stall at the compressor face measuring station. The cause of this delay is shown in the next figure.

Time histories of static pressure at the exit of the first seven stages of the eight-stage compressor are presented in figure 10 for the reading 2 stall point. The time interval, 0 to 50 milliseconds, corresponds to the same interval in the previous figure. Here each vertical division corresponds to about 3 milliseconds.

If each of these traces is examined closely, it is clear that the earliest "blip" in the stage exit pressure occurs at a time of 33 milliseconds. It is this time to which an instantaneous distortion peak should be related. The stall cell then rotates past the axial row of statics, and they appear to recover. At a time of about 41 milliseconds, the stall zone again wipes past the row of statics. This time increment corresponds to one revolution at about half-rotor speed. Complete flow breakdown, or terminal stall, is finally indicated by the row of interstage statics at t = 48 milliseconds. This is about 3 milliseconds after the first indication of stall hammershock was sensed by the compressor face probes.

The steady-state total pressure contour map corresponding to reading 3 is presented in figure 11. These data were recorded at Mach 2.6 at an inlet angle-of-attack of 6°. In contrast to reading 2, this distortion pattern is primarily circumferential, with the lower-pressure airflow in the bottom half of the inlet. Furthermore, the zones of highest dynamic activity for this reading occurred nearer the average and lower-pressure recovery regions. This resulted in some rather severe fluctuations of distortion amplitude, but the basic character of the distortion remained the same.

The time variation of distortion for reading 3 is shown in figure 12 over a 50-millisecond time span similar to that previously presented. The averaging time of 0.06 rotor revolution corresponds only to the effective averaging time of the pre-digitizer filters. Even with this short averaging time, the mean level of the fluctuating distortion is only about 10 percent higher than the steady-state distortion level. This is largely due to the predominant circumferential nature of the steady-state distortion. Like reading 2, this plot shows a large distortion peak which traverses above the critical level just prior to the earliest observation of compressor stall. This was probably the stall-inducing distortion peak, and because of its singularity and relation to compressor stall, an averaging time of about 0.07 rotor revolution is proper for this reading. This averaging time is only about 20 percent of that for reading 2.

CONCLUDING REMARKS.

Of 29 compressor stall points recorded in an investigation of supersonic inlet-engine compatibility, seven were extensively analyzed using the instantaneous distortion approach. Results indicate that this approach can be used to identify the unique distortion peak which is related to compressor stall. But the pressure averaging time required in this type analysis was found to vary considerably over the range of data analyzed. It may ultimately be necessary to use a mean averaging time in the evaluation of propulsion system compatibility, particularly for a system covering a wide range of operating conditions.

INLET-COLDPIPE INSTALLATION IN 10'×10' SWT

Figure 1

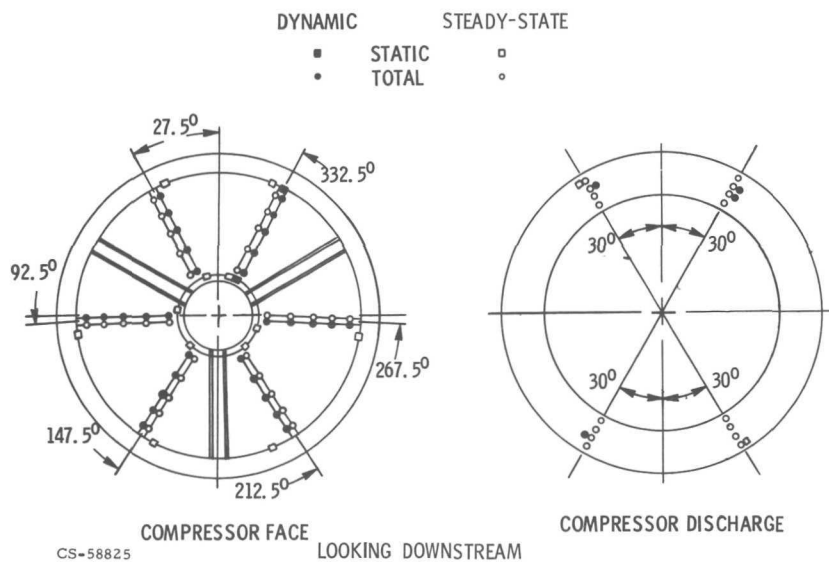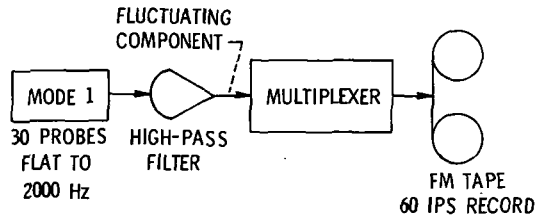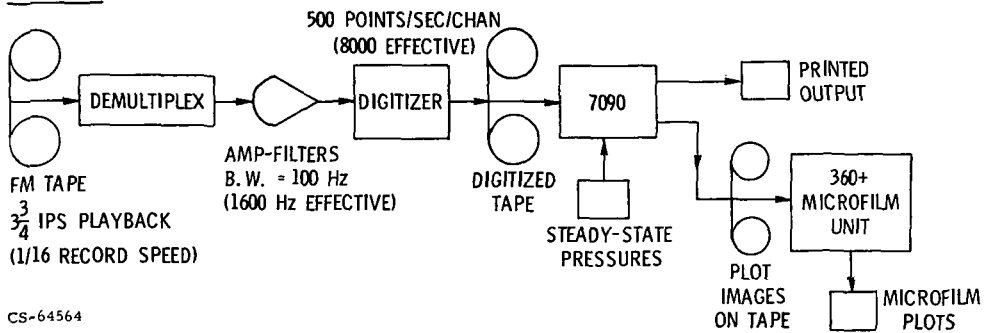## STEADY-STATE AND DYNAMIC PRESSURE INSTRUMENTATION

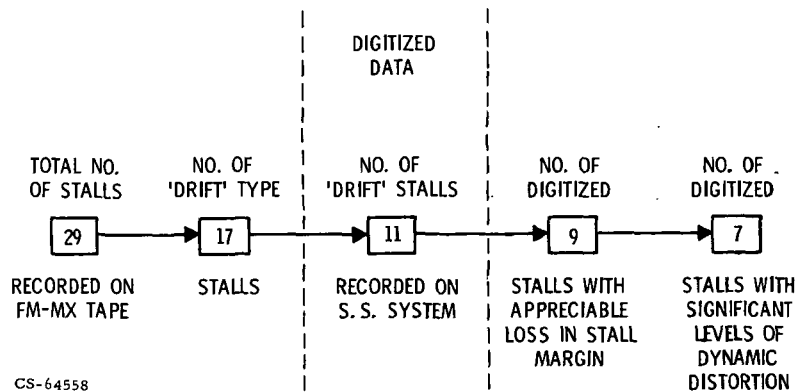Figure 2

DATA SYSTEMS

ACQUISITION

FLUCTUATING
COMPONENT ⌐

MODE 1 — ⟩ HIGH-PASS FILTER → MULTIPLEXER → FM TAPE 60 IPS RECORD

30 PROBES
FLAT TO
2000 Hz

HIGH-PASS
FILTER

REDUCTION

FM TAPE → DEMULTIPLEX → AMP-FILTERS B.W. = 100 Hz (1600 Hz EFFECTIVE) → DIGITIZER → 500 POINTS/SEC/CHAN (8000 EFFECTIVE)

FM TAPE
3¾ IPS PLAYBACK
(1/16 RECORD SPEED)

DIGITIZED TAPE → 7090 → PRINTED OUTPUT

STEADY-STATE PRESSURES

7090 → 360+ MICROFILM UNIT → MICROFILM PLOTS

PLOT IMAGES ON TAPE

CS-64564

Figure 3

DATA BANK RESULTING FROM 60/40 INLET - J85 ENGINE

COMPATIBILITY STUDY

DIGITIZED
DATA

TOTAL NO. OF STALLS	NO. OF 'DRIFT' TYPE	NO. OF 'DRIFT' STALLS	NO. OF DIGITIZED	NO. OF DIGITIZED
29	→ 17	→ 11	→ 9	→ 7
RECORDED ON FM-MX TAPE	STALLS	RECORDED ON S. S. SYSTEM	STALLS WITH APPRECIABLE LOSS IN STALL MARGIN	STALLS WITH SIGNIFICANT LEVELS OF DYNAMIC DISTORTION

CS-64558

Figure 4

STEADY-STATE DISTORTION CORRELATION

LOSS IN STALL PRESSURE RATIO

WEIGHTED DISTORTION INDEX, $\left(1 - \dfrac{P_{min,\,60^0}}{\bar{P}}\right) \times \sqrt{\dfrac{\beta}{\pi}}$
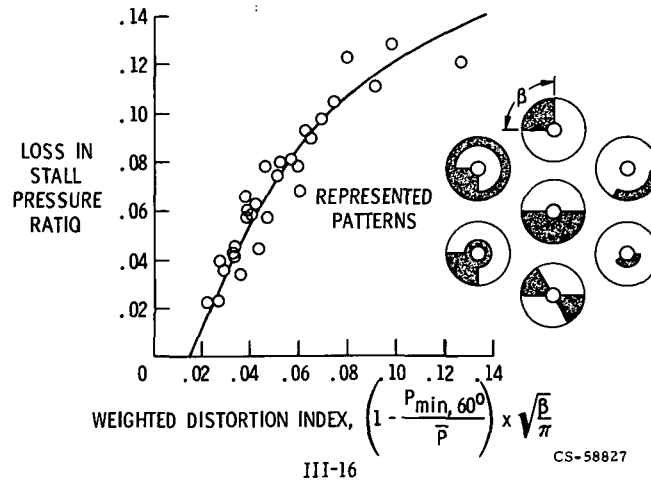
III-16

CS-58827

Figure 5

E-7329

SAMPLE OF DISTORTION VARIATION WITH TIME

INSTANTANEOUS-TO-CRITICAL DISTORTION RATIO = 1.26
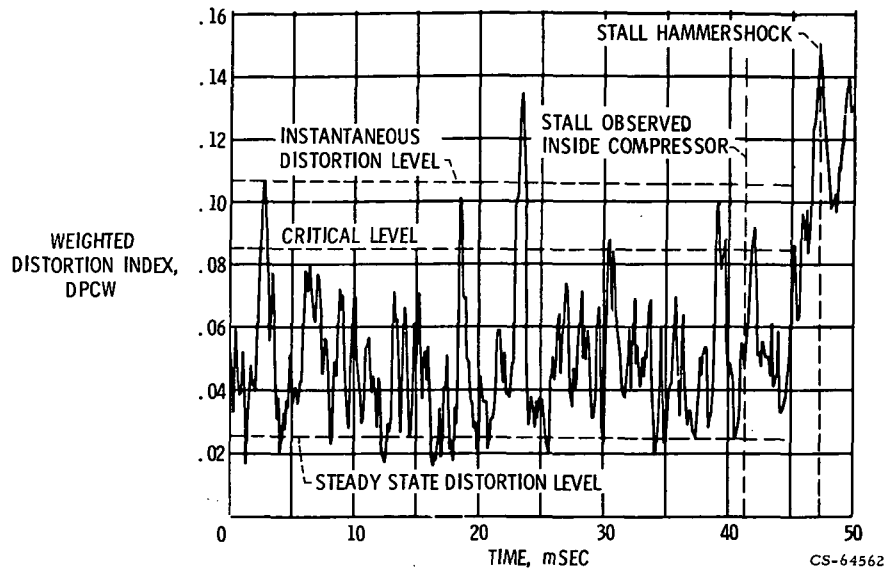
AVERAGING TIME = 0.072 ROTOR REVOLUTIONS

STALL HAMMERSHOCK

INSTANTANEOUS DISTORTION LEVEL

STALL OBSERVED INSIDE COMPRESSOR

CRITICAL LEVEL

WEIGHTED DISTORTION INDEX, DPCW

STEADY STATE DISTORTION LEVEL

TIME, mSEC

CS-64562

Figure 6

EFFECT OF AVERAGING TIME ON DISTORTION AMPLITUDE

CS-64560
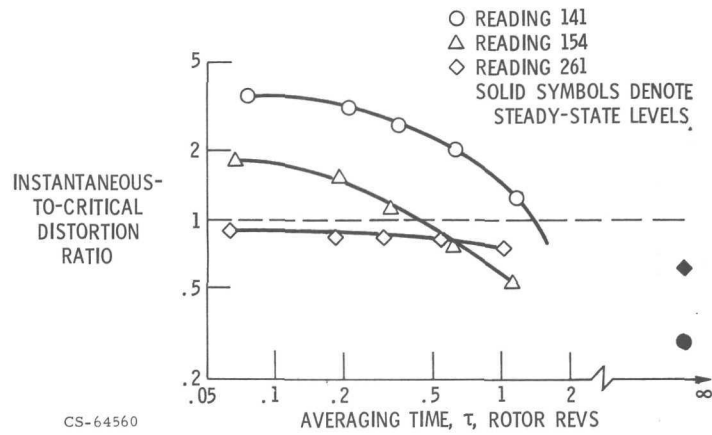
Figure 7

STEADY STATE DISTORTION CONTOURS
READING 154, $\overline{P}/P_0 = 0.799$

CS-64565

Figure 8

INSTANTANEOUS DISTORTION

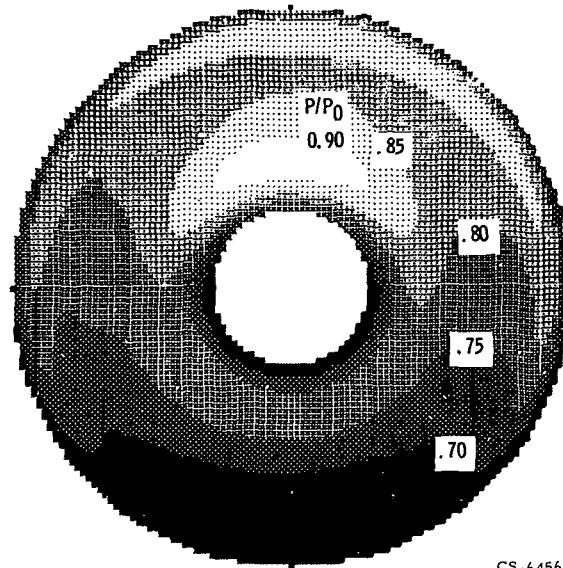READING 154, τ = 0.33 ROTOR REVOLUTIONS
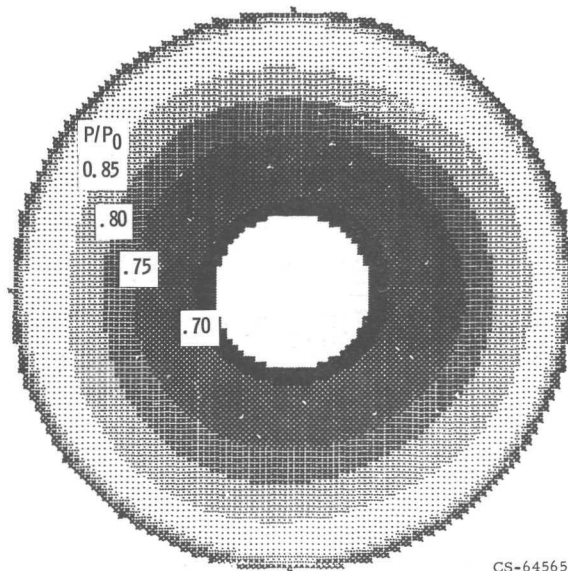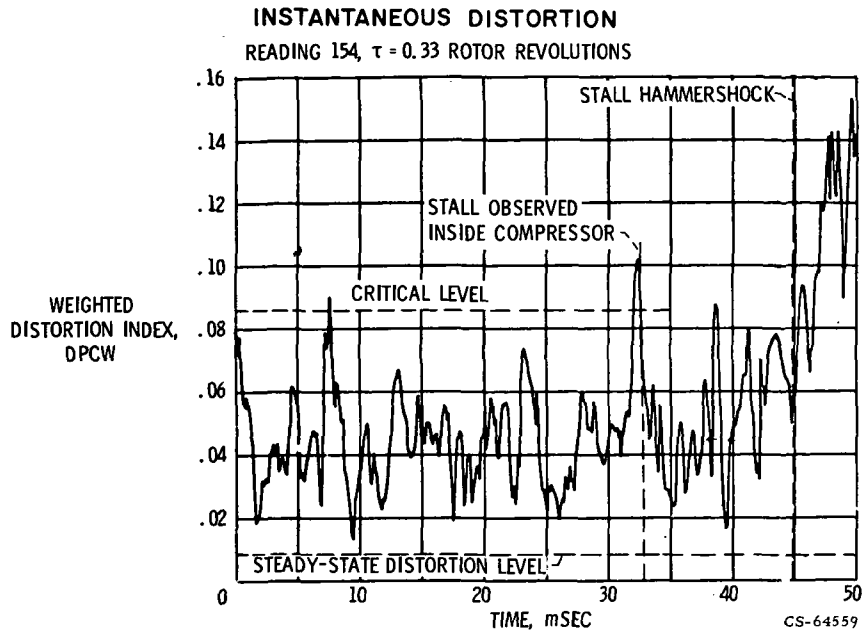
Figure 9

INTERSTAGE STATIC PRESSURE HISTORIES

READING 154
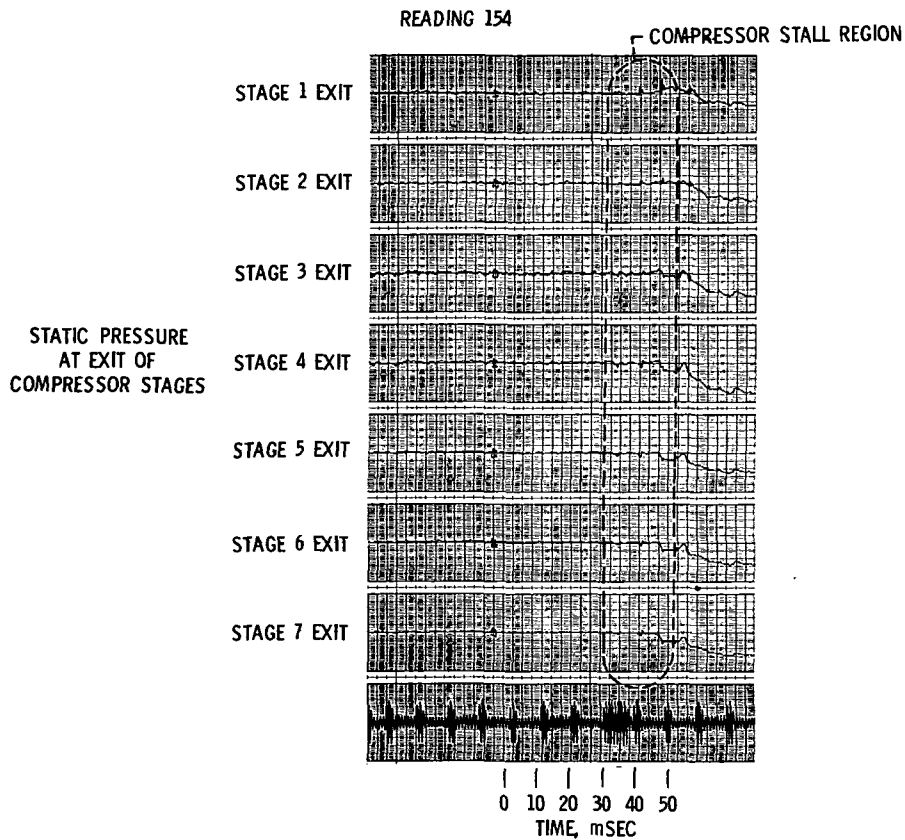
Figure 10

STEADY STATE DISTORTION CONTOURS
READING 261, $\bar{P}/P_0$ = 0.783

CS-64566

Figure 11

INSTANTANEOUS DISTORTION
READING 261, τ = 0.06 ROTOR REVOLUTIONS

Figure 12